
Trained Model in Supervised Deep Learning is a Conditional Risk Minimizer

Yutong Xie

Academy for Advanced Interdisciplinary Studies
Peking University
Beijing, 100871

Dufan Wu

MGH/BWH Center for Advanced Medical Computing and Analysis
Gordon Center for Medical Imaging, Department of Radiology
Massachusetts General Hospital and Harvard Medical School
Boston, MA 02114

Bin Dong

Beijing International Center for Mathematical Research
Peking University
Beijing, 100871
dongbin@bicmr.pku.edu.cn

Quanzheng Li

MGH/BWH Center for Advanced Medical Computing and Analysis
Gordon Center for Medical Imaging, Department of Radiology
Massachusetts General Hospital and Harvard Medical School
Boston, MA 02114
li.quanzheng@mgh.harvard.edu

Abstract

We proved that a trained model in supervised deep learning minimizes the conditional risk for each input (Theorem 2.1). This property provided insights into the behavior of trained models and established a connection between supervised and unsupervised learning in some cases. In addition, when the labels are intractable but can be written as a conditional risk minimizer, we proved an equivalent form of the original supervised learning problem with accessible labels (Theorem 2.2). We demonstrated that many existing works, such as Noise2Score, Noise2Noise and score function estimation can be explained by our theorem. Moreover, we derived a property of classification problem with noisy labels using Theorem 2.1 and validated it using MNIST dataset. Furthermore, We proposed a method to estimate uncertainty in image super-resolution based on Theorem 2.2 and validated it using ImageNet dataset. Our code is available on github¹.

1 Introduction

Supervised learning is one of the most widely-used paradigm in deep learning, where the network tries to learn a mapping from inputs to labels. In addition to the mapping itself, people are also

¹<https://github.com/Theodore-PKU/theorem-1-verification-python>.

interested in its properties, particularly under a posterior distribution, which is usually non-trivial and intractable. A common example is the supervised learning with noisy label. In practice it is almost impossible to get a clean label without any noise. Therefore, it is important to analyse the network’s behavior trained under noisy labels [Chen et al., 2019], and then design proper loss functions to eliminate the noises’ influence [Lehtinen et al., 2018]. Another example is the uncertainty estimation, where we are interested in predicting the conditional variance of network output [Kendall and Gal, 2017].

To describe how the trained network will behave when the dependency between labels and inputs is no longer deterministic but follows a non-trivial posterior distribution, we proposed a theorem (Theorem 2.1) which shows the trained networks will minimize the conditional risk with given network input. Based on this property, we can design a class of supervised learning methods with more accessible labels to solve challenging learning problems that have intractable labels (Theorem 2.2). A stronger conclusion was also given when the training loss is a L2 norm.

Many existing works related to noisy and intractable labels are special cases of our theory. Theoretical relationship was proved between the proposed methods and Noise2Noise, Noise2Score, and score function estimation [Lehtinen et al., 2018, Kim and Ye, 2021, Vincent, 2011]. Besides theoretical analysis, we further experimentally validated the proposed theorems on two problems: (1) MNIST classification with noisy labels in which we compared the network’s results with theoretically derived results; (2) uncertainty estimation of single image super-resolution in which we compared the uncertainty learned based on our theory with the one calculated by sampling the DDPM-SR model [Dhariwal and Nichol, 2021, Ho et al., 2020].

Our main contributions are: (1) we proved a trained model in supervised deep learning will minimize the conditional risk, which provided insights into the behavior of trained model and connected supervised and unsupervised learning in some cases; (2) we proposed a new training strategy for supervised learning when labels are intractable, and proved the equivalence between the original learning problem and the new training strategy. (3) Our theorems explained many existing works and was applied to analyze image classification models trained with noisy labels and uncertainty estimation of single image super-resolution.

This paper is organized as follows. In Section 2 we give the main theorems, build theoretical relationship between proposed methods and existing works. We introduce the details of two verification tasks in Section 3. Experiment results of them are shown in Section 4. At last, we show the related works in Section 5 and conclusion in Section 6.

Table 1: The concrete meanings of the same notations in different scenarios.

SCENARIO	INPUT: y	VARIABLE: x	LABEL: $g(x, y)$	LOSS: L
IMAGE CLASSIFICATION	IMAGE	ONE-HOT VECTOR	x	CROSS-ENTROPY
NOISE2SCORE	NOISY IMAGE	CLEAN IMAGE	x	L2 NORM
NOISE2NOISE	NOISY IMAGE	NOISY IMAGE	x	L2 NORM
SCORE FUNCTION ESTIMATION	RANDOM VARIABLE	RANDOM VARIABLE	$\nabla_y \log p(y x)$	L2 NORM
UNCERTAINTY ESTIMATION IN SUPER-RESOLUTION	LOW-RESOLUTION IMAGE	HIGH-RESOLUTION IMAGE	x OR $(x - \mathbb{E}_{x y}[x])^2$	L2 NORM

2 Theory

2.1 Notation

We will generally use y for input and $g(x, y)$ for labels. We use more general form $g(x, y)$ instead of x to denote labels in order to cover a wide range of applications in this work. In most cases (particularly related to Theorem 2.1) $g(x, y) = x$ and x is the label. In some cases related to Theorem 2.2 $g(x, y)$ could be a more complicated function. To avoid confusion, the definition of major notations under

different scenarios is summarized in Table 1, which will also be further explained again in each section.

2.2 Understanding Model Trained in Supervised Learning

In this section we consider a general case of supervised learning in which the labels follow a distribution conditioned on the inputs. To understand what the model will learn under this scenario, we propose the following Theorem 2.1:

Theorem 2.1. *Assuming that X, Y and W are measurable spaces; x and y are random variables defined in X and Y respectively; $g(x, y) : X \times Y \rightarrow W$ is a measurable function; $L(a, b) : W \times W \rightarrow \mathbb{R}$ is a loss function which satisfies $L(a, b) \geq L(a, a)$ and $L(a, b) \geq L(b, b)$; $f(y; \theta) : Y \rightarrow W$ is a model parameterized by θ and for any measurable function $\tilde{f}(y) : Y \rightarrow W$, there exists some θ such that $f(\cdot; \theta) = \tilde{f}(\cdot)$. Then the optimal solution θ^* to the following problem:*

$$\min_{\theta} \mathbb{E}_{x,y} [L(f(y; \theta), g(x, y))], \quad (1)$$

satisfies that $f(y; \theta^*) = z^*(y)$ where

$$z^*(y) = \arg \min_z \mathbb{E}_{x|y} [L(z, g(x, y))]. \quad (2)$$

The proof of Theorem 2.1 is in Appendix A.1. In addition, a more generalized form of Theorem 2.1 without the parameterized model is given in Appendix A.2.

Theorem 2.1 states that for a supervised learning problem $y \rightarrow g(x, y)$, the learned model $f(y; \theta^*)$ is equal to $z^*(y)$, a conditional risk minimizer. $z^*(y)$ is selected so that the loss between $z^*(y)$ and the labels $g(x, y)$ is minimized over the conditional distribution $x | y$. Theorem 2.1 will be trivial if there exists a mapping from y to x , and the trained model will be a data fitting process from y to $g(x, y)$ in this case (see Appendix A.3).

Noting that $z^*(y)$ is a function of y and is connected to the conditional distribution $x | y$ instead of specific labels $g(x, y)$, Theorem 2.1 implies two applications. (1) *analyzing the behavior of trained model*: when the label $g(x, y)$ follows a probability distribution (e.g. noisy label), we can analyze the property of the trained model $f(y; \theta^*)$ through $z^*(y)$; (2) *connecting supervised and unsupervised learning*: if $z^*(y)$ can be directly estimated from the dataset of inputs $\{y\}$, the model obtained by supervised learning can be trained from $\{y\}$ using unsupervised learning without labels $g(x, y)$.

2.2.1 Image classification with noisy labels

Image classification with noisy labels is an example of the first application. In this case, y represents the image to be classified, x is the one-hot vector of image class, $g(x, y) = x$ is the label, and L is cross-entropy loss. When labels are correct, there exists a mapping from y to x and we can map y to the right category based on the optimal model $f(y; \theta^*)$. However, if the annotation of dataset is inaccurate and noisy, Theorem 2.1 can be used to analyze the behavior of $f(y; \theta^*)$ through $z^*(y)$. Given the noisy label distribution $p(x | y)$, one can calculate $z^*(y)$ according to Equation (2). Examples of different label noise distributions will be given in Section 3.1 with their corresponding experimental results in Section 4.1.

2.2.2 Noise2Score

Noise2Score [Kim and Ye, 2021] is an example of the second application. It is an unsupervised learning method for image denoising task. In this scenario, x is the clean image, $y = x + n$ is the noisy image with noise n , $g(x, y) = x$ is the label, and L is L2 norm loss. Supervised learning by Equation (1) leads to $z^*(y) = \mathbb{E}_{x|y}[x]^2$. If n follows an exponential family distribution, according to the Tweedie’s formula [Efron, 2011, Robbins, 2020], $\mathbb{E}_{x|y}[x]$ has a closed form and is related to $\nabla_y \log p(y)$, the score function of y . For instance, $\mathbb{E}_{x|y}[x] = y + \sigma^2 \nabla_y \log p(y)$ if $n \sim \mathcal{N}(0, \sigma^2 I)$. In Noise2Score, $\nabla_y \log p(y)$ is estimated by AR-DAE [Lim et al., 2020] where only $\{y\}$ is used. Therefore, $z^*(y)$ can be learned using only $\{y\}$ and thus the original supervised learning problem is converted to unsupervised learning.

²The proof is in Appendix A.4.

2.3 Equivalent Training Target for Intractable Labels

There are a class of deep learning problems that could be considered as to train a network to predict the minimal conditional risk $z^*(y)$. However, $z^*(y)$ could be very difficult to compute or even intractable. In this case we propose the following Theorem 2.2 which shows that one can train the model using labels $g(x, y)$ instead. Furthermore, a stronger conclusion on the equivalency can be drawn under L2 norm.

Theorem 2.2. *Given all the assumptions in Theorem 2.1 and a target function $z^*(y) : Y \rightarrow W$ which satisfies that:*

$$z^*(y) = \arg \min_z \mathbb{E}_{x|y} [L(z, g(x, y))], \quad (3)$$

then the following equation holds:

$$\arg \min_{\theta} \mathbb{E}_y [L(f(y; \theta), z^*(y))] = \arg \min_{\theta} \mathbb{E}_{x,y} [L(f(y; \theta), g(x, y))]. \quad (4)$$

If L is L2 norm loss, we further have that $z^*(y) = \mathbb{E}_{x|y} [g(x, y)]$ and for any model $f(y; \theta) : Y \rightarrow W$, the following equation holds:

$$\mathbb{E}_y \|f(y; \theta) - z^*(y)\|_2^2 + C = \mathbb{E}_{x,y} \|f(y; \theta) - g(x, y)\|_2^2,$$

where C is a constant. Therefore, the following two optimization problems are equivalent:

$$\min_{\theta} \mathbb{E}_y \|f(y; \theta) - z^*(y)\|_2^2 \iff \min_{\theta} \mathbb{E}_{x,y} \|f(y; \theta) - g(x, y)\|_2^2. \quad (5)$$

The proof of Theorem 2.2 is in Appendix A.5.

Equation (4) implies that one can achieve the same model by using either $z^*(y)$ or $g(x, y)$ as labels, which is extremely powerful when $z^*(y)$ is intractable. For example, $z^*(y)$ needs to be calculated by averaging over the conditional distribution $x | y$. Usually we only have one sample of x for each y , which prevents the direct calculation of $z^*(y)$. Theorem 2.2 tells us that we can use $g(x, y)$ as labels, which relies on single pairs of x and y , instead. When L2 norm is used as loss function, it is a special case of Equation (4). Under L2 norm, the two object functions are differed by merely a constant. Hence, not only the final optimal solutions will be the same, but also any intermediate solutions during the optimization, e.g. if the training is early stopped.

In the following subsections, we will show that Noise2Noise and current method to estimate score function are special cases of Theorem 2.2; we will also apply Theorem 2.2 to compute uncertainty of single image super-resolution.

2.3.1 Noise2Noise

Noise2Noise [Lehtinen et al., 2018] claims that one can train a denoising model by mapping a noisy image to another noisy image, where the two images share the same content but independent noises. In this case, let $y = s + n_1$ and $x = s + n_2$, where s is the underlying clean image, n_1 and n_2 are two independent noises. Let $g(x, y) = x$ and L be the L2 norm, we have:

$$z^*(y) = \arg \min_z \mathbb{E}_{x|y} \|z - x\|_2^2 = \mathbb{E}_{x|y} [x]. \quad (6)$$

From Theorem 2.2, we have:

$$\min_{\theta} \mathbb{E}_{x,y} \|f(y; \theta) - x\|_2^2 \iff \min_{\theta} \mathbb{E}_y \|f(y; \theta) - \mathbb{E}_{x|y} [x]\|_2^2. \quad (7)$$

On the other hand, let $x = s$ and we can similarly get that:

$$\min_{\theta} \mathbb{E}_{s,y} \|f(y; \theta) - s\|_2^2 \iff \min_{\theta} \mathbb{E}_y \|f(y; \theta) - \mathbb{E}_{s|y} [s]\|_2^2. \quad (8)$$

If n_2 is zero mean, we have

$$\mathbb{E}_{x|y} [x] = \mathbb{E}_{s|y} [s]. \quad (9)$$

The proof to equations (7), (8), and (9) are given in Appendix A.6. Combining equations (7), (8), and (9) gives the equivalence between training with x and s , which is the Noise2Noise training:

$$\min_{\theta} \mathbb{E}_{x,y} \|f(y; \theta) - x\|_2^2 \iff \min_{\theta} \mathbb{E}_{s,y} \|f(y; \theta) - s\|_2^2$$

In summary, Theorem 2.2 helped to build the connection between the intractable target s and the noisy labels x through $z^*(y)$, which explained how the Noise2Noise training works.

2.3.2 Score Function Estimation

Estimation of the score function is essential in some applications such as image denoising and generation [Kim and Ye, 2021, Song et al., 2020]. For a random variable y , its score function is defined as $\nabla_y \log p(y)$. Let y and x be two random variables, Vincent [2011] has proved that:

$$\min_{\theta} \mathbb{E}_y \left[\|f(y; \theta) - \nabla_y \log p(y)\|_2^2 \right] \iff \min_{\theta} \mathbb{E}_{x,y} \left[\|f(y; \theta) - \nabla_y \log p(y | x)\|_2^2 \right]. \quad (10)$$

$\nabla_y \log p(y)$ is usually inaccessible but $\nabla_y \log p(y | x)$ can sometimes be computed by selecting appropriate x . Equation (10) indicates that the score function $\nabla_y \log p(y)$ can be estimated using the substituted labels $\nabla_y \log p(y | x)$; this equation is the basis of all score function based methods.

Theorem 2.2 provides a simple alternative proof to Equation (10). Let $g(x, y) = \nabla_y \log p(y | x)$ and L be the L2 norm loss, we have

$$\begin{aligned} z^*(y) &= \arg \min_z \mathbb{E}_{x|y} \|z - g(x, y)\|_2^2 = \mathbb{E}_{x|y} [g(x, y)] \\ &= \mathbb{E}_{x|y} [\nabla_y \log p(y | x)] = \nabla_y \log p(y). \end{aligned} \quad (11)$$

Hence, $z^*(y)$ provides the left hand side of Equation (10) and $g(x, y)$ provides its right hand side, and the equivalence in Equation (10) is proved according to Theorem 2.2. The proof to Equation (11) is give in Appendix A.7.

2.3.3 Uncertainty Estimation of Single Image Super-Resolution

Theorem 2.2 can be further applied to the uncertainty estimation of single image super-resolution. In this case, x is a high-resolution image and y is the corresponding low-resolution image. Let $z^*(y)$ be some data uncertainty we want to estimate over the conditional distribution $x | y$, which is intractable because the conditional distribution is unknown. However, if we can find suitable $g(x, y)$ and L such that $z^*(y)$ satisfies Equation (3), $z^*(y)$ can be estimated using $g(x, y)$ as the training label. For example, for pixel-wise variance, our target $z^*(y)$ is $\mathbb{E}_{x|y} (x - \mathbb{E}_{x|y}[x])^2$, which satisfies Equation (3) when $g(x, y) = (x - \mathbb{E}_{x|y}[x])^2$ and L is the L2 norm loss. More details are in Section 3.2.

2.4 Summary

So far, we introduced our main theoretical results and their relation to previous works. Theorem 2.1 characterizes the property of trained model in supervised learning problem given by Equation (1). One can analyze the behavior of the trained model through $z^*(y)$, which gives insights into noisy label problems, as demonstrated in Section 3.1. Based on Theorem 2.1, a supervised learning problem can also be converted to unsupervised learning problem if one can fit $z^*(y)$ from the inputs $\{y\}$ as shown in Noise2Score.

Theorem 2.2 states the equivalence between the two training approaches, where one can convert the intractable labels $z^*(y)$ to the tractable ones $g(x, y)$. We found that it explains previous works including Noise2Noise and score function estimation. We further applied it to uncertainty estimation of single image super-resolution as in Section 3.2.

The successes of previous works, including Noise2Score, Noise2Noise, and score function estimation confirmed the proposed theorems. In the following sections, we will further verify our theorems and demonstrate their utility for practical applications by carrying out experiments on two tasks: image classification with noisy labels and uncertainty estimation of single image super-resolution.

3 Two Verification Tasks as Examples of Practical Applications

In this section, we discuss two verification tasks in detail, which are examples of practical applications of our theorems: (1) image classification with noisy labels, where Theorem 2.1 is used to analyze the trained model’s behavior through $z^*(y)$; (2) uncertainty estimation of single image super-resolution, where Theorem 2.2 is used to perform supervised learning when the labels are intractable.

3.1 Image Classification with Noisy Labels

Suppose there are n classes for classification, y is the image to be classified, and x represents an n -dimensional one-hot vector of image class c where $c \in \{1, 2, \dots, n\}$ and the components of x are all 0 but 1 at the position c . Usually, $g(x, y) = x$ is the label, L is cross-entropy loss $\text{CE}(\cdot, \cdot)$, and the classification model $f(y; \theta)$ is trained by:

$$\min_{\theta} \mathbb{E}_{x,y} [\text{CE}(f(y; \theta), x)]. \quad (12)$$

The output of $f(y; \theta)$ is also an n -dimensional vector representing the predictive probabilities for each class. During inference, usually the class with the highest predictive probability will be chosen as the classification result. If the labels are correct, the optimal model $f(y; \theta^*)$, i.e. $z^*(y)$, will map y to the one-hot vector x and predict the right category³.

When the labels are noisy, the annotations of y may be wrong and is sampled from $\{1, 2, \dots, n\}$ following a discrete distribution. Without loss of generality, we assume that the noise distribution is dependent on y . We denote the distribution as an n -dimensional vector q_y , which satisfies that $\sum_{i=1}^n q_{y,i} = 1$ and $q_{y,i} \geq 0$. $q_{y,i}$ is the i th element of q_y and represents the probability that y is labeled as class i . $z^*(y)$ in Theorem 2.1 can be calculated as:

$$z^*(y) = \arg \min_z \mathbb{E}_{x|y} [\text{CE}(z, x)] = q_y. \quad (13)$$

The proof of Equation (13) is in Appendix A.8. Equation (13) shows that the optimal model $f(y; \theta^*)$ trained by noisy labels will map y to q_y . In other word, the predictive probability distribution of $f(y; \theta^*)$ is exactly the label noise distribution. Assuming the model performs the same on the testing and training datasets, and the class with the highest predictive probability is used, Equation (13) indicates that different label noise distributions q_y may affect the testing accuracy differently.

We consider three different label noise distribution q_y to experimentally verify Theorem 2.1. Let $x^{(i)}$ represent the one-hot vector corresponding to class i . Given y and its correct class c , we define the three types of label noise as follows:

1. *Uniform noise*: there is equal possibility to misclassify y to any incorrect class,

$$q_{y,i} = p(x^{(i)} | y) = \begin{cases} \alpha & \text{if } i = c, \\ \frac{1-\alpha}{n-1} & \text{if } i \neq c. \end{cases} \quad (14)$$

where $0 < \alpha < 1$ is the probability of correct classification.

2. *Biased noise*: y may only be misclassified to a neighboring class,

$$q_{y,i} = p(x^{(i)} | y) = \begin{cases} \alpha & \text{if } i = c, \\ 1 - \alpha & \text{if } i = c+1, \\ 0 & \text{otherwise.} \end{cases} \quad (15)$$

where $c_{+1} = (c + 1) \bmod n$ and $0 < \alpha < 1$ is the probability of correct classification.

3. *Generated noise*: assuming there is another trained classification model $M(y)$ whose output is also a predictive probabilities for each class, q_y is defined as follows,

$$q_{y,i} = p(x^{(i)} | y) = \begin{cases} \beta M(y)_c & \text{if } i = c, \\ \frac{1-\beta M(y)_c}{1-M(y)_c} M(y)_i & \text{if } i \neq c. \end{cases} \quad (16)$$

where $M(y)_i$ represents the predictive probability of class i and $0 < \beta < 1$. We assume that softmax operation is used in $M(y)$, therefore $M(y)_c < 1$ and Equation (16) is well defined.

Uniform noise and biased noise are class-dependent whereas generated noise is instance-dependent, i.e. q_y is different for different samples. Experimental details and results are shown in Section 4.1.

³Practically, because the output of f is usually the result of softmax operation, the predictive probabilities are all larger than 0. Therefore, output of $f(y; \theta^*)$ will be very close to x .

3.2 Uncertainty Estimation of Single Image Super-resolution

Let x be a high-resolution image and y be the corresponding low-resolution image. They satisfy $y = Ax$ where A is a down-sampling operator. Given y there are many x that share the same low-resolution image y because A is underdetermined. Hence, it is worth to measure the uncertainty of the super-resolved images given y to estimate how reliable it is. The uncertainty here is defined as a value that can be calculated from the statistical distribution $x | y$. For example, the most widely used pixel-wise variance is defined as:

$$\text{Var}_{x|y} [x] = \mathbb{E}_{x|y} (x - \mathbb{E}_{x|y}[x])^2 \quad (17)$$

Normally the uncertainty cannot be calculated directly because $x | y$ is unknown. An alternative method is the Monte Carlo approach where a generative super-resolution model is used to generate multiple samples from $x | y$ to calculate the statistics [Dhariwal and Nichol, 2021]. However, it is time-consuming and the accuracy extremely depends on the performance of generative model.

Theorem 2.2 can be used to solve the uncertainty estimation problem. As discussed in Section 2.3.3, let $z^*(y) = \text{Var}_{x|y} [x]$, $g(x, y) = (x - \mathbb{E}_{x|y} [x])^2$, and L be the L2 norm loss, we can train a model to learn the pixel-wise variance using:

$$\min_{\theta} \mathbb{E}_{x,y} \|f(y; \theta) - (x - \mathbb{E}_{x|y}[x])^2\|_2^2. \quad (18)$$

Note that $\mathbb{E}_{x|y}[x]$ is still intractable but we can apply Theorem 2.2 again to train a mean-estimating model:

$$\min_{\theta_1} \mathbb{E}_{x,y} \|f_{\text{mean}}(y; \theta_1) - x\|_2^2, \quad (19)$$

and $f_{\text{mean}}(y, \theta_1)$ will fit to $\mathbb{E}_{x|y}[x]$. Then we can substitute $\mathbb{E}_{x|y}[x]$ in Equation (18) with $f_{\text{mean}}(y, \theta_1)$ and train the variance-estimating model:

$$\min_{\theta_2} \mathbb{E}_{x,y} \|f_{\text{var}}(y; \theta_2) - (x - f_{\text{mean}}(y; \theta_1))^2\|_2^2. \quad (20)$$

Details and results of relevant experiments are given in Section 4.2. Some other statistics on $x | y$ as listed in Appendix B.2 Table 5 may be estimated in the similar way, but they are remained for future works.

4 Experiments

The notations in Section 4.1 and Section 4.2 are the same to Section 3.1 and Section 3.2, respectively.

4.1 Image Classification with Noisy Labels

4.1.1 Experiment Setup

We conducted the experiment on MNIST dataset [LeCun, 1998], which contains 60k images of 10 digits, from 0 to 9. The noisy labels were constructed as follows: for each y , we sampled c from q_y once and (y, c) was used as a training pair. Several groups of the hyperparameters α and β were selected to model different noise levels, where in each group different noise types shared the same ratio of correct labels η . To effectively match the noise levels, we set β from 0.2 to 0.9 with an interval of 0.1. For each β , we first calculated the correct label rate η of the generated noise, then set $\alpha = \eta$ because $\mathbb{E}[\eta] = \alpha$ for uniform and biased noise. The specific values of α and β are listed in Appendix B.1 Table 4.

A CNN with two convolutional layers and three fully-connected layers was used as the classification model $f(y; \theta)$. We trained $f(y; \theta)$ for 20k iterations with a batch size of 128. Adam optimizer with learning rate of 0.0001 was used. M was trained in the same manner but without label noise. The models were saved every 2k iterations and we selected the ones with the minimal loss as final models, since we focus on the optimal model of Equation (12).

To verify Equation (13), we need to evaluate the closeness between the predictive probabilities of trained model $f(y; \theta^*)$ and q_y . We computed the average of cross-entropy loss over the training set:

$$\overline{\text{CE}}_f = \frac{1}{N} \sum_{i=1}^N \text{CE}(f(y; \theta^*), q_y), \quad (21)$$

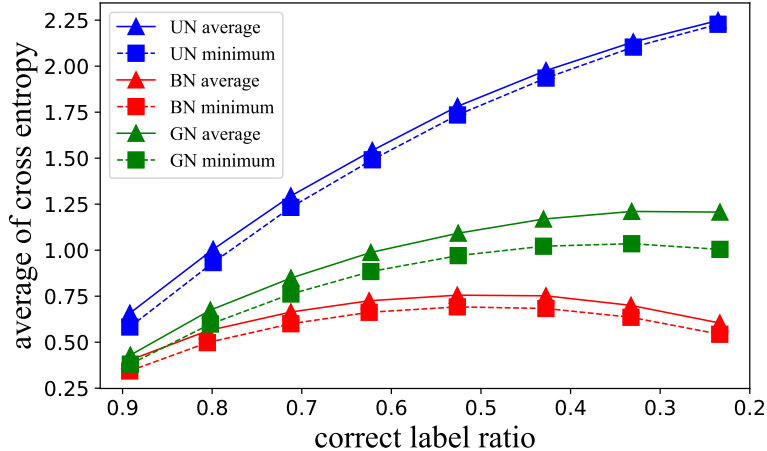


Figure 1: The comparison between \overline{CE}_f and \overline{CE}_q for three types of label noise. The solid lines represent \overline{CE}_f and the dash lines represent \overline{CE}_q . UN: uniform noise; BN: biased noise; GN: generated noise.

and compared it to the theoretical minimum value

$$\overline{CE}_q = \frac{1}{N} \sum_{i=1}^N CE(q_y, q_y), \quad (22)$$

where N is the size of the training set. In addition, we use the accuracy of classification over test set to evaluate and compare the performance of models trained by different types of noisy labels.

4.1.2 Experiment Results

Figure 1 shows that \overline{CE}_f and \overline{CE}_q follows the same trend and have small margins at different noise levels for all three types of noises due to the limit of dataset size and imperfect training. It verifies that the predictive probabilities of the trained model is close to the theoretical results q_y . In Figure 2, we further show the predictive probabilities and q_y for digit 5 and $\beta = 0.6$. The averages of all images of digit 5 are listed in the left column and three instances are listed in the right column. It can be seen that the model predictions (red lines) and the calculated q_y (green lines) are in good accordance with each other for both the averaged and individual curves, which further verified our theoretical result in Equation (13). More results are given in Appendix C.1 Figure 5, Figure 6 and Figure 7.

The accuracy of classification at different noise levels is illustrated in Figure 3, which demonstrates the different behavior of the trained models under different noise distributions. Uniform noise has little influence on the accuracy. It is because that we were taking the maximum element of q_y as the prediction, but in uniform noise, it needs $\alpha < 0.1$ for the probability of the incorrect classes to surpass that of the correct class in q_y . For the biased noise type, it only requires that $\alpha < 0.5$ for that to happen, and that is why the accuracy with biased noise drops drastically at the correct label rate of 0.5. For generated noise, it is easier than uniform noise for the magnitude of the wrong classes in q_y to surpass the correct ones, but it is harder than the biased noise. Hence the generated noise has an accuracy curve in between.

4.1.3 Discussion

The experiment provides evidence and explanation to deep learning’s resilience to label noises, which is unavoidable in practical applications. As demonstrated in Figure 3, the trained models had very decent performance at a labeling error rate of 30% for all three noise levels. Because the model has different resilience to noise levels under different noise types, it is important to understand the type of labeling noises and design appropriate quality assurance procedure accordingly. For example,

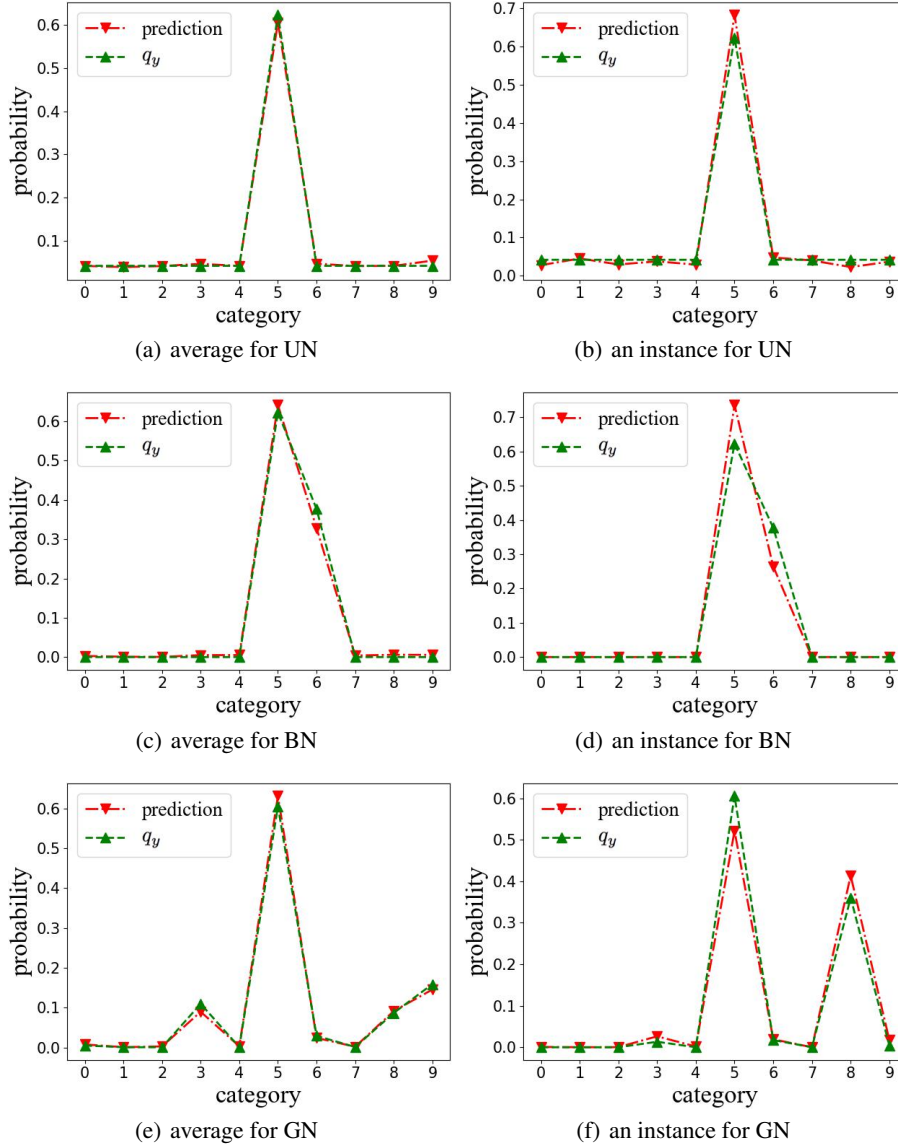


Figure 2: The predicted probabilities by the trained models compared to q_y for digit 5 at $\beta = 0.6$. The left column is the average for all images of digit 5. The right column plots a single instance. The red lines represent $f(y; \theta)$ whereas the green lines represent q_y . UN: uniform noise; BN: biased noise; GN: generated noise.

if the labels are derived from automatically collected data it may suffer from uniform noise due to measurement errors, and the model can tolerate higher label noise level. However, for manually annotated data the label noise may be closer to generated noise (recognition error) or biased noise (misoperation during labeling), where we need to pay more attention to the correctness of the label because the model is less resistant to labeling noises.

4.2 Pixel-wise Variance Estimation of Single Image Super-resolution

4.2.1 Experiment Setup

We conducted an experiment on the ImageNet dataset [Deng et al., 2009], which contains 1.28 million images of 1k categories. We randomly chose 2 images from each category in the original training set

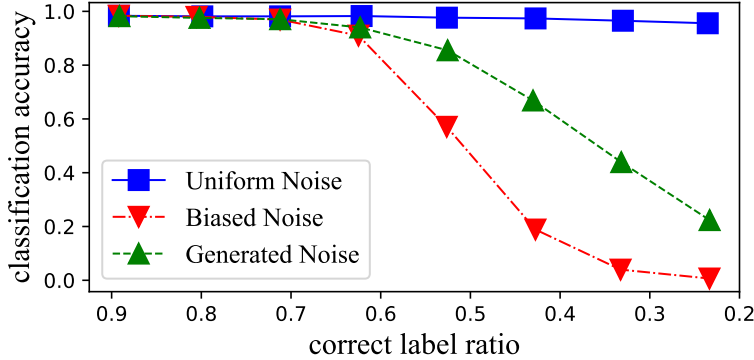


Figure 3: The accuracies of classification on test data for three types of label noise and different noise level.

for testing, whereas the remaining images were used for training. The task was $4\times$ super-resolution from 64×64 to 256×256 . As reference, we employed an SR model based on DDPM to generate multiple high-resolution images given a low-resolution input [Dhariwal and Nichol, 2021, Ho et al., 2020]. Some generated samples are given in Appendix C.2 Figure 10. The mean and pixel-wise variance of $x | y$ were estimated by the Monte Carlo method using 100 samples. For convenience, we call this model DDPM-SR.

For our proposed direct estimation method, the network architecture of f_{mean} and f_{var} was modified from DDPM-SR by removing the embedding part of time t and categorical information. Because the network architecture is similar to a U-Net [Ronneberger et al., 2015], we upsampled y to 256×256 resolution as the input of networks. A smaller network compared to DDPM-SR was also adopted to reduce the training time.

We first trained $f_{\text{mean}}(\cdot; \theta_1)$ by Equation (19), followed by training $f_{\text{var}}(\cdot; \theta_2)$ by Equation (20). During the training of the variance network, we concatenated $f_{\text{mean}}(y; \theta_1)$ with y along the channel dimension and fed it as the input to f_{var} . We trained $f_{\text{mean}}(\cdot; \theta_1)$ for 90k steps and $f_{\text{var}}(\cdot; \theta_2)$ for 50k steps with a batch size of 64. The AdamW optimizer with learning rate of 0.0001 was used for both f_{mean} and f_{var} . The models at the end of training iterations were selected as the final models.

PSNR, MSE, and NMSE were used to evaluate the models’ performance. We used the squared root of the pixel-wise variance, i.e. pixel-wise standard deviation to compute these metrics.

4.2.2 Experiment Result

The quantitative comparison among x , DDPM-SR and the proposed direct estimation are given in Table 2. For the mean estimation, f_{mean} is much closer to the mean estimated from DDPM-SR compared to the high-resolution image x , which verifies that $f_{\text{mean}}(\cdot; \theta_1)$ trained by Equation (19) fits to the conditional expectation $\mathbb{E}_{x|y}[x]$ instead of the target x . This also explains the smoothness that people observed when training SR models with L2 norm loss. The directly estimated variance f_{var} is also very close to the variance calculated from DDPM-SR, with a very small NMSE of 0.1145.

An instance is given in Figure 4. As expected, $f_{\text{mean}}(y; \theta_1)$ is smoother than x since it is predicting the conditional expectation instead of x . The pixel-wise variance from $f_{\text{var}}(y; \theta_2)$ and DDPM-SR are visually very close to each other. The training label, $|x - \mathbb{E}_{x|y}[x]|$, is also given in the figure and demonstrates huge difference from the estimated variance, which indicates that the proposed model would fit to the uncertainty instead of single data points. More examples are given in Appendix C.2 Figure 8 and Figure 9.

4.2.3 Discussion

Experimental results demonstrated the feasibility of using our method to estimate the uncertainty in single image super-resolution. Compared to the generative model, the proposed model trades

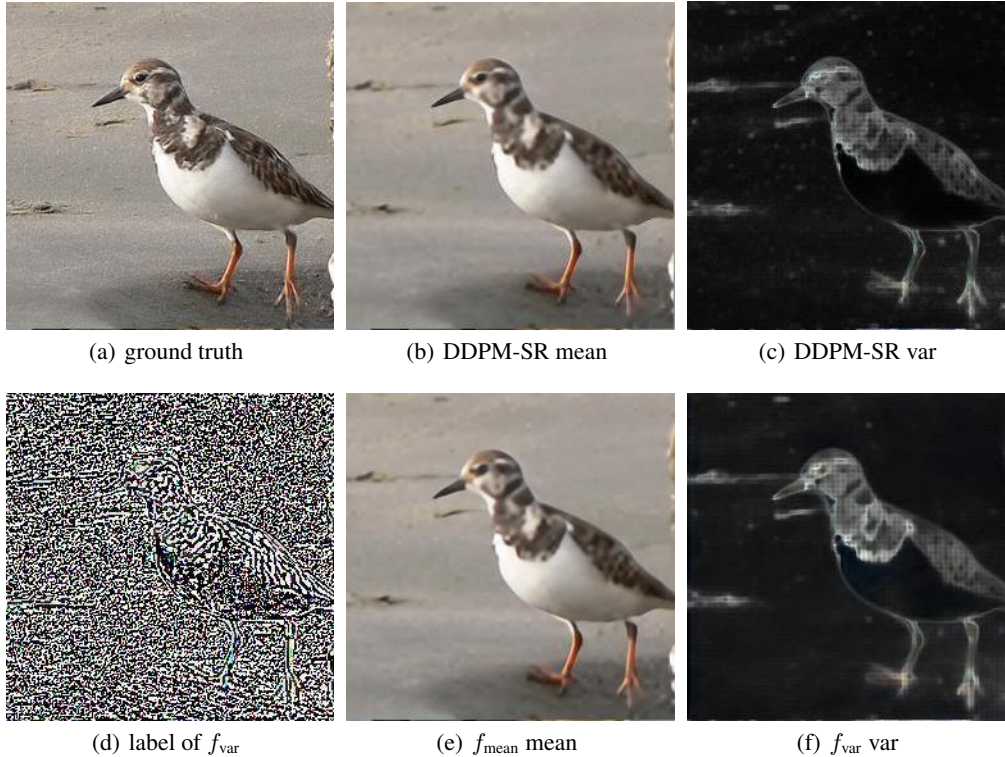


Figure 4: Images: (a) the high-resolution image x ; (b) estimated $\mathbb{E}_{x|y}[x]$ by DDPM-SR; (c) estimated pixel-wise standard deviation by DDPM-SR; (d) square root of label when training f_{var} , i.e. $|x - \mathbb{E}_{x|y}[x]|$; (e) estimated $\mathbb{E}_{x|y}[x]$ by f_{mean} ; (f) estimated pixel-wise standard deviation by f_{var} . Images in the bottom row are rescaled for better display.

Table 2: Evaluation metrics. The latter one of comparison objects is regarded as reference when computing. DDPM-SR stands for the mean or variance calculated from 100 samples depending on the comparing results.

METRICS	PSNR (\uparrow)	MSE (\downarrow)	NMSE (\downarrow)
DDPM-SR vs x	27.6426	37.3984	2.5395
f_{MEAN} vs x	27.3060	38.3413	2.2611
f_{MEAN} vs DDPM-SR	37.4526	9.7725	1.0446
f_{VAR} vs DDPM-SR	23.9540	15.0560	0.1145

flexibility for speed during inference. In practice, we may only need one sample of the super-resolved images accompanied by the uncertainty (pixel-wise variance) map, and the proposed method will avoid the high computational cost required by the Monte Carlo sampling.

The proposed method can be easily modified to compute the expected error of a trained deterministic SR model against the ground truth x , where one can replace the f_{mean} in Equation (20) with the trained target model. Beyond variance, it is also possible to train other statistical values such as skewness as listed in Appendix C.2 Table 5. In addition, this method can be also applied to other inverse problem, including denoising, deblurring, and image reconstruction.

5 Related Works

Theoretical results and experiments in this paper are related to many previous works in different areas, including unsupervised denoising [Lehtinen et al., 2018, Kim and Ye, 2021], score function

estimation [Hyvärinen and Dayan, 2005, Vincent, 2011, Song et al., 2020], classification with noisy labels [Arpit et al., 2017, Rolnick et al., 2017, Chen et al., 2019], uncertainty estimation of inverse problem [Adler and Öktem, 2018].

In Theorem 2.1, when $g(x, y) = x$ and L is L2 norm loss, Equation (1) is the least squares regression problem whose optimal solution, $\mathbb{E}_{x|y}[x]$, is well-known [Murphy, 2012]. It has been used to explain why the trained model by L2 norm loss tends to predict a smooth result in many low-level vision tasks. Adler and Öktem [2018] expanded the result with more general $g(x, y)$ under L2 norm loss, which is the stronger conclusion of Theorem 2.1. The relationship between supervised learning and unsupervised learning for image denoising task was also discussed in Noise2Score [Kim and Ye, 2021].

Noise2Noise [Lehtinen et al., 2018] was proposed to train a denoising model when clean images are inaccessible, which is an application of Theorem 2.2. Score function is an important concept in statistics [Robbins, 2020, Efron, 2011] and its estimation is used in generative models recently [Hyvärinen and Dayan, 2005, Song et al., 2020]. Vincent [2011] proved the equivalence of Equation (10) and many works follows the training strategy [Song et al., 2020]. Theorem 2.2 provided an alternative proof to Equation (10).

Classification with noisy labels has been studied in many works [Arpit et al., 2017, Rolnick et al., 2017, Chen et al., 2019]. Chen et al. [2019] claimed that when the classification model is trained by labels with class-dependent noise, the predictive probability follows the same distribution as the label noise, which is a special case of our analysis in Section 3.1. Our experiment in Section 4.1 is similar to the ones conducted in [Rolnick et al., 2017] and our experiment results are consistent to theirs. Adler and Öktem [2018] also proposed a method to estimate the pixel-wise variance in computed tomography (CT) reconstruction.

6 Conclusion

In this work, we first proved that a trained model in supervised deep learning minimizes the conditional risk for each input. We then illustrated the equivalence between supervised learning problems with intractable labels and its computationally feasible substitution. In addition, we explained many different existing works, such as Noise2Score, Noise2Noise and score function estimation through our theorems. In addition, by applying our theorems we showed that the predictive probability of image classification models trained with noisy labels is related to the noise distribution theoretically and experimentally. Furthermore, we proposed and validated a method to accurately estimate uncertainty of single image super-resolution based on our theorems.

References

- Pengfei Chen, Ben Ben Liao, Guangyong Chen, and Shengyu Zhang. Understanding and utilizing deep neural networks trained with noisy labels. In *International Conference on Machine Learning*, pages 1062–1070. PMLR, 2019.
- Jaakko Lehtinen, Jacob Munkberg, Jon Hasselgren, Samuli Laine, Tero Karras, Miika Aittala, and Timo Aila. Noise2noise: Learning image restoration without clean data. *arXiv preprint arXiv:1803.04189*, 2018.
- Alex Kendall and Yarin Gal. What uncertainties do we need in bayesian deep learning for computer vision? In I. Guyon, U. V. Luxburg, S. Bengio, H. Wallach, R. Fergus, S. Vishwanathan, and R. Garnett, editors, *Advances in Neural Information Processing Systems*, volume 30. Curran Associates, Inc., 2017. URL <https://proceedings.neurips.cc/paper/2017/file/2650d6089a6d640c5e85b2b88265dc2b-Paper.pdf>.
- Kwanyoung Kim and Jong Chul Ye. Noise2score: Tweedie’s approach to self-supervised image denoising without clean images. *arXiv preprint arXiv:2106.07009*, 2021.
- Pascal Vincent. A connection between score matching and denoising autoencoders. *Neural computation*, 23(7):1661–1674, 2011.
- Prafulla Dhariwal and Alex Nichol. Diffusion models beat gans on image synthesis. *arXiv preprint arXiv:2105.05233*, 2021.

- Jonathan Ho, Ajay Jain, and Pieter Abbeel. Denoising diffusion probabilistic models. *arXiv preprint arXiv:2006.11239*, 2020.
- Bradley Efron. Tweedie’s formula and selection bias. *Journal of the American Statistical Association*, 106(496):1602–1614, 2011.
- Herbert Robbins. *An empirical Bayes approach to statistics*. University of California Press, 2020.
- Jae Hyun Lim, Aaron Courville, Christopher Pal, and Chin-Wei Huang. Ar-dae: Towards unbiased neural entropy gradient estimation. In *International Conference on Machine Learning*, pages 6061–6071. PMLR, 2020.
- Yang Song, Jascha Sohl-Dickstein, Diederik P Kingma, Abhishek Kumar, Stefano Ermon, and Ben Poole. Score-based generative modeling through stochastic differential equations. *arXiv preprint arXiv:2011.13456*, 2020.
- Yann LeCun. The mnist database of handwritten digits. <http://yann.lecun.com/exdb/mnist/>, 1998.
- Jia Deng, Wei Dong, Richard Socher, Li-Jia Li, Kai Li, and Li Fei-Fei. Imagenet: A large-scale hierarchical image database. In *2009 IEEE conference on computer vision and pattern recognition*, pages 248–255. Ieee, 2009.
- Olaf Ronneberger, Philipp Fischer, and Thomas Brox. U-net: Convolutional networks for biomedical image segmentation. In *International Conference on Medical image computing and computer-assisted intervention*, pages 234–241. Springer, 2015.
- Aapo Hyvärinen and Peter Dayan. Estimation of non-normalized statistical models by score matching. *Journal of Machine Learning Research*, 6(4), 2005.
- Devansh Arpit, Stanisław Jastrzębski, Nicolas Ballas, David Krueger, Emmanuel Bengio, Maxinder S Kanwal, Tegan Maharaj, Asja Fischer, Aaron Courville, Yoshua Bengio, et al. A closer look at memorization in deep networks. In *International Conference on Machine Learning*, pages 233–242. PMLR, 2017.
- David Rolnick, Andreas Veit, Serge Belongie, and Nir Shavit. Deep learning is robust to massive label noise. *arXiv preprint arXiv:1705.10694*, 2017.
- Jonas Adler and Ozan Öktem. Deep bayesian inversion. *arXiv preprint arXiv:1811.05910*, 2018.
- Kevin P Murphy. *Machine learning: a probabilistic perspective*. MIT press, 2012.

A Proofs

A.1 Proof of Theorem 2.1

Proof. For any θ and function $f(\cdot; \theta)$, we have that:

$$\begin{aligned} \mathbb{E}_{x,y} [L(f(y; \theta), g(x, y))] &= \mathbb{E}_y [\mathbb{E}_{x|y} [L(f(y; \theta), g(x, y))]] \\ &\geq \mathbb{E}_y \left[\min_z \mathbb{E}_{x|y} [L(z, g(x, y))] \right] \\ &= \mathbb{E}_y \left[\mathbb{E}_{x|y} \left[L \left(\arg \min_z \mathbb{E}_{x|y} [L(z, g(x, y))], g(x, y) \right) \right] \right] \\ &= \mathbb{E}_{x,y} \left[L \left(\arg \min_z \mathbb{E}_{x|y} [L(z, g(x, y))], g(x, y) \right) \right]. \end{aligned}$$

Let $z^*(y) = \arg \min_z \mathbb{E}_{x|y} [L(z, g(x, y))]$. According to the assumption of $f(\cdot; \theta)$, there exists θ^* such that $f(y; \theta^*) = z^*(y)$ which is the optimal solution. \square

A.2 Another Version of Theorem 2.1

Theorem A.1. *Assume that:*

- X, Y and W are measurable spaces;
- x and y are random variables defined in X and Y respectively;
- $g(x, y) : X \times Y \rightarrow W$ is a measurable function;
- $L(a, b) : W \times W \rightarrow \mathbb{R}$ is a loss function and satisfies that

$$L(a, b) \geq L(a, a), L(a, b) \geq L(b, b). \quad (23)$$

- $f(y) : Y \rightarrow W$ is a measurable function.

Consider the following optimization problem:

$$\min_f \mathbb{E}_{x,y} [L(f(y), g(x, y))], \quad (24)$$

the optimal solution f^* satisfies:

$$f^*(y) = z^*(y) = \arg \min_z \mathbb{E}_{x|y} [L(z, g(x, y))]. \quad (25)$$

A.3 The derivation of $z^*(y) = g(x, y)$ when there exists a mapping from y and x

Suppose $x = h(y)$, we have that

$$p(x | y) = \begin{cases} 1, & \text{if } x = h(y) \\ 0 & \text{otherwise} \end{cases}$$

Then, we derive that

$$z^*(y) = \arg \min_z \mathbb{E}_{x|y} [L(z, g(x, y))] = \arg \min_z [L(z, g(x, y))] = g(x, y)$$

Therefore, $z^*(y) = g(x, y)$ holds.

A.4 Proof of $z^*(y) = \mathbb{E}_{x|y}[x]$

Proof. For any z , we have that

$$\begin{aligned} \mathbb{E}_{x|y} \left[\|z - x\|_2^2 \right] &= \mathbb{E}_{x|y} \left[\|z - \mathbb{E}_{x|y}[x] + \mathbb{E}_{x|y}[x] - x\|_2^2 \right] \\ &= \mathbb{E}_{x|y} \left[\|z - \mathbb{E}_{x|y}[x]\|_2^2 + 2 \langle z - \mathbb{E}_{x|y}[x], \mathbb{E}_{x|y}[x] - x \rangle + \|\mathbb{E}_{x|y}[x] - x\|_2^2 \right] \\ &\geq \mathbb{E}_{x|y} \left[\|\mathbb{E}_{x|y}[x] - x\|_2^2 \right] + 2 \mathbb{E}_{x|y} \left[\langle z - \mathbb{E}_{x|y}[x], \mathbb{E}_{x|y}[x] - x \rangle \right] \\ &= \mathbb{E}_{x|y} \left[\|\mathbb{E}_{x|y}[x] - x\|_2^2 \right]. \end{aligned}$$

The last equality holds because

$$\begin{aligned}
\mathbb{E}_{x|y} [\langle z - \mathbb{E}_{x|y} [x], \mathbb{E}_{x|y} [x] - x \rangle] &= \langle z - \mathbb{E}_{x|y} [x], \mathbb{E}_{x|y} [\mathbb{E}_{x|y} [x] - x] \rangle \\
&= \langle z - \mathbb{E}_{x|y} [x], \mathbb{E}_{x|y} [x] - \mathbb{E}_{x|y} [x] \rangle \\
&= \langle z - \mathbb{E}_{x|y} [x], 0 \rangle \\
&= 0.
\end{aligned}$$

Therefore,

$$\arg \min_z \mathbb{E}_{x|y} [\|z - x\|_2^2] = \mathbb{E}_{x|y} [x].$$

□

A.5 Proof of Theorem 2.2

Proof. According to Theorem 2.1, the optimal solution of $\min_{\theta} \mathbb{E}_{x,y} [L(f(y; \theta), g(x, y))]$, θ^* , satisfies that $f(y; \theta^*) = z^*(y)$. For any θ , we have

$$\mathbb{E}_y [L(f(y; \theta), z^*(y))] \geq \mathbb{E}_y [L(z^*(y), z^*(y))] = \mathbb{E}_y [L(f(y; \theta^*), z^*(y))].$$

That is to say, θ^* is also the optimal solution of $\min_{\theta} \mathbb{E}_y [L(f(y; \theta), z^*(y))]$. Therefore, Equation (4) holds.

Similar to the proof in Appendix A.4, we can prove that

$$\arg \min_z \mathbb{E}_{x|y} [\|z - g(x, y)\|_2^2] = \mathbb{E}_{x|y} [g(x, y)].$$

Then, we can derive that:

$$\begin{aligned}
&\mathbb{E}_y [\|f(y; \theta) - z^*(y)\|_2^2] - \mathbb{E}_{x,y} [\|f(y; \theta) - g(x, y)\|_2^2] \\
&= \mathbb{E}_y [\|f(y; \theta)\|_2^2] - 2\mathbb{E}_y [\langle f(y; \theta), \mathbb{E}_{x|y} [g(x, y)] \rangle] + \mathbb{E}_y [\|\mathbb{E}_{x|y} [g(x, y)]\|_2^2] - \mathbb{E}_{x,y} [\|f(y; \theta)\|_2^2] \\
&\quad + 2\mathbb{E}_{x,y} [\langle f(y; \theta), g(x, y) \rangle] - \mathbb{E}_{x,y} [\|g(x, y)\|_2^2] \\
&= -2\mathbb{E}_y [\langle f(y; \theta), \mathbb{E}_{x|y} [g(x, y)] \rangle] + C_1 + 2\mathbb{E}_{x,y} [\langle f(y; \theta), g(x, y) \rangle] - C_2,
\end{aligned}$$

where $\mathbb{E}_y [\|\mathbb{E}_{x|y} [g(x, y)]\|_2^2]$ and $\mathbb{E}_{x,y} [\|g(x, y)\|_2^2]$ are constants denoted as C_1 and C_2 respectively.

Because

$$\begin{aligned}
\mathbb{E}_{x,y} [\langle f(y; \theta), g(x, y) \rangle] &= \int \int p(x, y) \langle f(y; \theta), g(x, y) \rangle dx dy \\
&= \int \int p(y) p(x | y) \langle f(y; \theta), g(x, y) \rangle dx dy \\
&= \int \int p(y) \langle f(y; \theta), p(x | y) g(x, y) \rangle dx dy \\
&= \int p(y) \left(\int \langle f(y; \theta), p(x | y) g(x, y) \rangle dx \right) dy \\
&= \int p(y) \left\langle f(y; \theta), \int p(x | y) g(x, y) dx \right\rangle dy \\
&= \int p(y) \langle f(y; \theta), \mathbb{E}_{x|y} [g(x, y)] \rangle dy \\
&= \mathbb{E}_y [\langle f(y; \theta), \mathbb{E}_{x|y} [g(x, y)] \rangle],
\end{aligned}$$

we have that

$$\mathbb{E}_y [\|f(y; \theta) - f^*(y)\|_2^2] - \mathbb{E}_{x,y} [\|f(y; \theta) - g(x, y)\|_2^2] = C_1 - C_2.$$

Let $C = C_2 - C_1$, then the following equation holds:

$$\mathbb{E}_y [\|f(y; \theta) - z^*(y)\|_2^2] + C = \mathbb{E}_{x,y} [\|f(y; \theta) - g(x, y)\|_2^2],$$

where C is a constant. Therefore, Equation (5) is proved. □

A.6 Proof of Equation (7), Equation (8) and Equation (9)

Proof. Let $g(x, y) = x$, then Equation (7) holds according to Theorem 2.2. Equation (8) is proved as long as replacing x in Equation (7) by s .

Next, we prove Equation (9). Suppose n_2 is sampled from a random variable n , which represents the noise. Because $\mathbb{E}[n] = 0$, then

$$\mathbb{E}_{x|s}[x] = \mathbb{E}_n[s + n] = s.$$

We can derive that

$$\begin{aligned} \mathbb{E}_{x|y}[x] &= \int p(x | y)x dx \\ &= \int \left(\int p(x, s | y) ds \right) x dx \\ &= \int \left(\int p(x | s, y)p(s | y) ds \right) x dx \\ &= \int \left(\int p(x | s)p(s | y) ds \right) x dx \\ &= \int p(s | y) \left(\int p(x | s)x dx \right) ds \\ &= \int p(s | y)\mathbb{E}_{x|s}[x] ds \\ &= \int p(s | y)s ds \\ &= \mathbb{E}_{s|y}[s]. \end{aligned}$$

Thus, Equation (9) holds. □

A.7 Proof of Equation (11)

Proof. We only need to prove that $\mathbb{E}_{x|y}[\nabla_y \log p(y | x)] = \nabla_y \log p(y)$. We have the following derivation:

$$\begin{aligned} \mathbb{E}_{x|y}[\nabla_y \log p(y | x)] &= \int p(x | y)\nabla_y \log p(y | x) dx \\ &= \int p(x | y)\nabla_y \log \frac{p(x | y)p(y)}{p(x)} dx \\ &= \int p(x | y)\nabla_y [\log p(x | y) + \log p(y) - \log p(x)] dx \\ &= \int p(x | y)\nabla_y \log p(x | y) dx + \int p(x | y)\nabla_y \log p(y) dx \\ &= \int p(x | y)\nabla_y \log p(x | y) dx + \nabla_y \log p(y). \end{aligned}$$

Next, we prove that $\int p(x | y)\nabla_y \log p(x | y) dx = 0$.

$$\begin{aligned} \int p(x | y)\nabla_y \log p(x | y) dx &= \int p(x | y) \frac{1}{p(x | y)} \nabla_y p(x | y) dx \\ &= \int \nabla_y p(x | y) dx \\ &= \nabla_y \int p(x | y) dx \\ &= \nabla_y 1 = 0. \end{aligned}$$

Thus, Equation (11) is proved. □

A.8 Proof of Equation Equation (13)

Proof. When cross-entropy loss $\text{CE}(a, b)$ for two discrete distributions is computed, two inputs, a and b , must satisfy that $\sum_{i=1}^n a_i = \sum_{i=1}^n b_i = 1$, and for any i , $a_i \geq 0, b_i \geq 0$. Otherwise cross-entropy loss cannot measure the closeness of two discrete distributions. Rigorously, when at least one input does not satisfy the condition, we can define $\text{CE}(a, b) = +\infty$. In addition, we define $0 \log 0 = 0$ since $\lim_{x \rightarrow 0} x \log x = 0$ according to L'Hospital's rule. Therefore, $\arg \min_z \mathbb{E}_{x|y} [\text{CE}(z, x)]$ can be rewritten as the the following optimization problem:

$$\begin{aligned} & \arg \min_z \mathbb{E}_{x|y} [\text{CE}(z, x)] \\ \text{s.t } & \sum_{i=1}^n z_i = 1, \\ & z_i \geq 0, i = 1, \dots, n. \end{aligned} \tag{26}$$

We denote the n -dimension one-hot vector whose components are all 0 but 1 at the position i as $x^{(i)}$. Suppose z satisfies the constraints. Since $p(x = x^{(i)} | y) = q_{y,i}$, we have that

$$\mathbb{E}_{x|y} [\text{CE}(z, x)] = \sum_{i=1}^n q_{y,i} \sum_{j=1}^n -x_j^{(i)} \log z_j = - \sum_{i=1}^n q_{y,i} \log z_i. \tag{27}$$

Bring Equation (27) to the optimization problem Equation (26) and solve it by the Lagrange multiplier method. We derive that

$$\arg \min_z \mathbb{E}_{x|y} [\text{CE}(z, x)] = q_y.$$

□

B More details of Experiments

B.1 Details for Image Classification with Noisy Labels

The CNN network architecture and concrete parameters are listed in Table 3. The digit image is scaled to range of $[0, 1]$ by dividing 255. The specific values of α and β for different noise level are listed in Table 4.

Table 3: Parameters of CNN

LAYER	PARAMETERS
CONV	6 CHANNELS, STRIDE IS 5
RELU	NONE
MAX POOLING	NONE
CONV	16 CHANNELS, STRIDE IS 5
RELU	NONE
MAX POOLING	NONE
FLATTEN	NONE
LINEAR	OUTPUT DIMENSION IS 128
RELU	NONE
LINEAR	OUTPUT DIMENSION IS 64
RELU	NONE
LINEAR	OUTPUT DIMENSION IS 10

B.2 Details for Pixel-wise Variance Estimation of Single Image Super-resolution

Table 5 lists some examples of statistics that can be represented by $\mathbb{E}_{x|y} [g(x, y)]$.

Our code of this experiment was based on Dhariwal et al.'s code⁴ [Dhariwal and Nichol, 2021]. We use the default parameters provided by their code except that we only used 4 times down-sampling.

⁴<https://github.com/openai/guided-diffusion>

Table 4: The values of α and β at different noise levels and corresponding correct label ratio for three types noise labels.

NOISE TYPE	UNIFORM	BIAS	GENERATED
$\alpha = 0.8913, \beta = 0.9$	0.8919	0.8920	0.8913
$\alpha = 0.7121, \beta = 0.7$	0.7122	0.7122	0.7121
$\alpha = 0.5254, \beta = 0.5$	0.5262	0.5264	0.5254
$\alpha = 0.4302, \beta = 0.4$	0.4274	0.4275	0.4302
$\alpha = 0.3318, \beta = 0.3$	0.3300	0.3326	0.3318

Table 5: Examples of statistics represented by $\mathbb{E}_{x|y} [g(x, y)]$.

STATISTICS	$g(x, y)$
MEAN	x
COVARIANCE MATRIX	$(x - \mathbb{E}_{x y} [x]) (x - \mathbb{E}_{x y} [x])^T$
PIXEL-WISE VARIANCE	$(x - \mathbb{E}_{x y} [x])^2$
PIXEL-WISE SKEWNESS	$\frac{(x - \mathbb{E}_{x y} [x])^3}{\mathbb{E}_{x y} [(x - \mathbb{E}_{x y} [x])^2]^{3/2}}$

We also utilized mixed precision to accelerate computing. To avoid f_{var} outputs values less than 0, we replaced those values by 0.

C More Results of Experiments

C.1 Image Classification with Noisy Labels

We show more comparison between predictive probability and q_y for uniform noise, biased noise and generated noise in Figure 5, Figure 6 and Figure 7, respectively.

C.2 Pixel-wise Variance Estimation of Single Image Super-resolution

We show more results of DDPM-SR, f_{mean} and f_{var} in Figure 8 and Figure 9. To illustrate the image quality of DDPM-SR, we show some super-resolution samples in Figure 10.

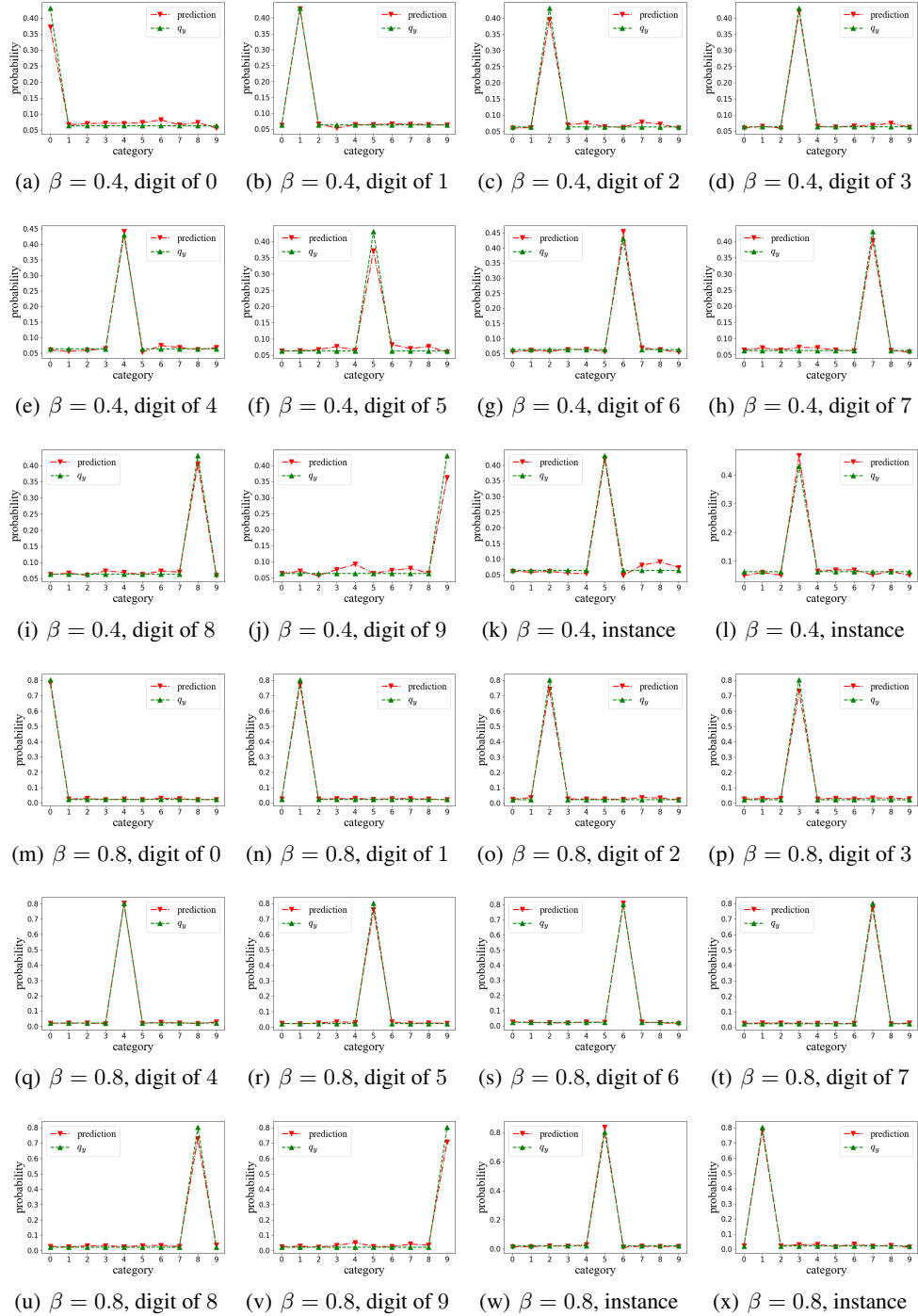


Figure 5: Uniform noise when $\beta = 0.4$ and $\beta = 0.8$. (k), (l), (w) and (x): instances of digit 5. Others are the average of predicted probabilities and q_y for all images of different digits. The red lines represent $f(y; \theta)$ whereas the green lines represent q_y .

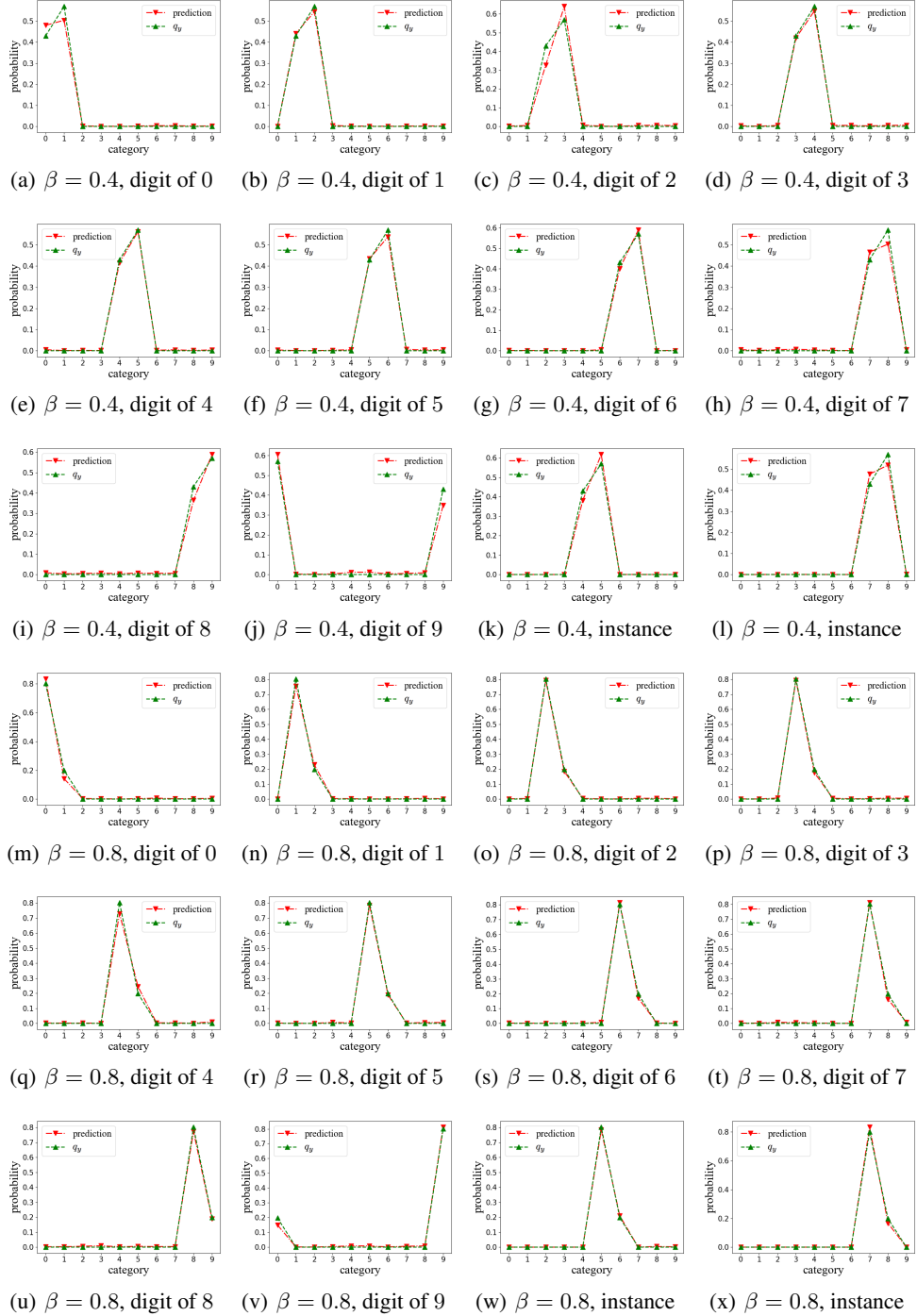


Figure 6: Biased noise when $\beta = 0.4$ and $\beta = 0.8$. (k), (l), (w) and (x): instances of digit 5. Others are the average of predicted probabilities and q_y for all images of different digits. The red lines represent $f(y; \theta)$ whereas the green lines represent q_y .

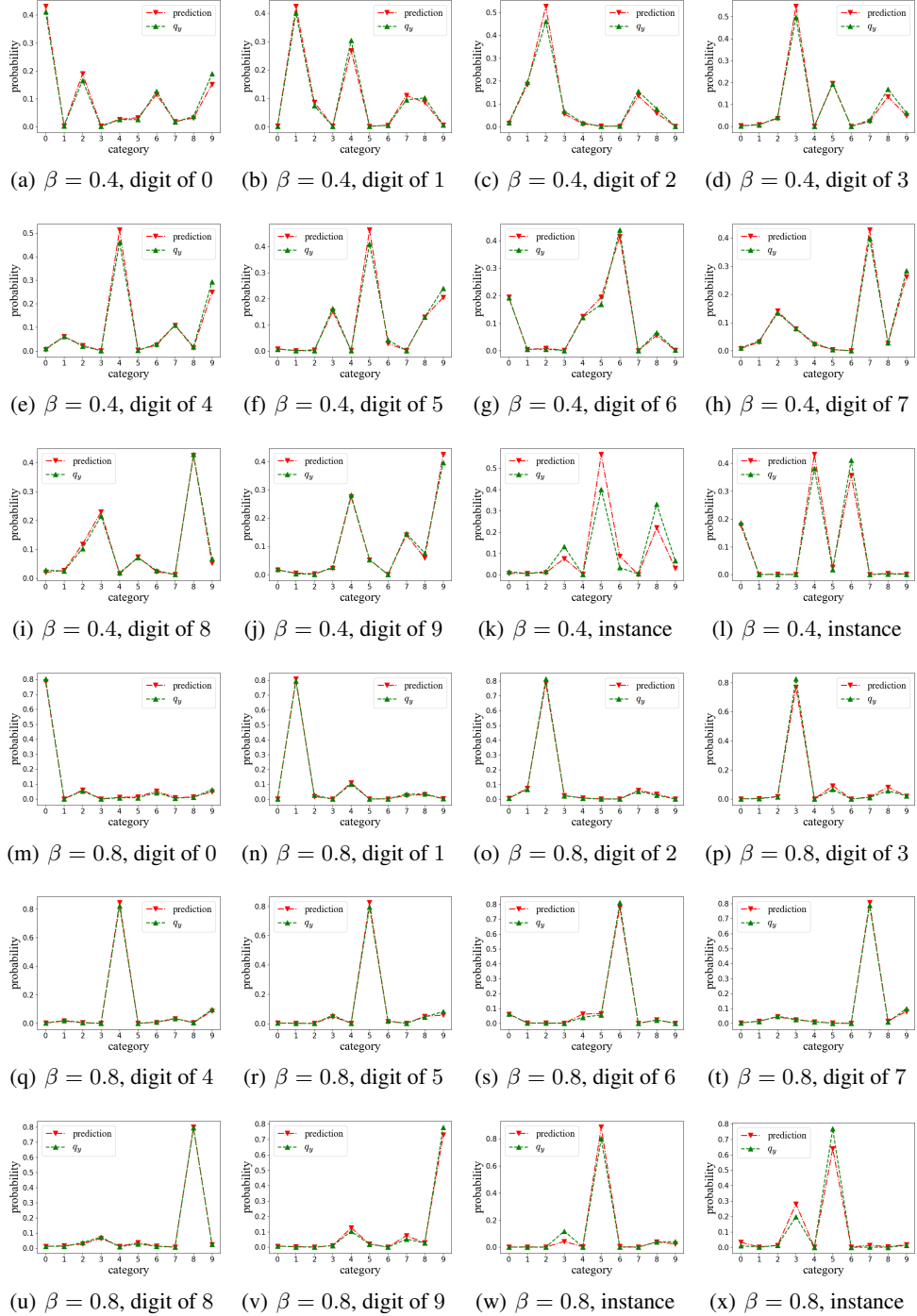


Figure 7: Generated noise when $\beta = 0.4$ and $\beta = 0.8$. (k), (l), (w) and (x): instances of digit 5. Others are the average of predicted probabilities and q_y for all images of different digits. The red lines represent $f(y; \theta)$ whereas the green lines represent q_y .

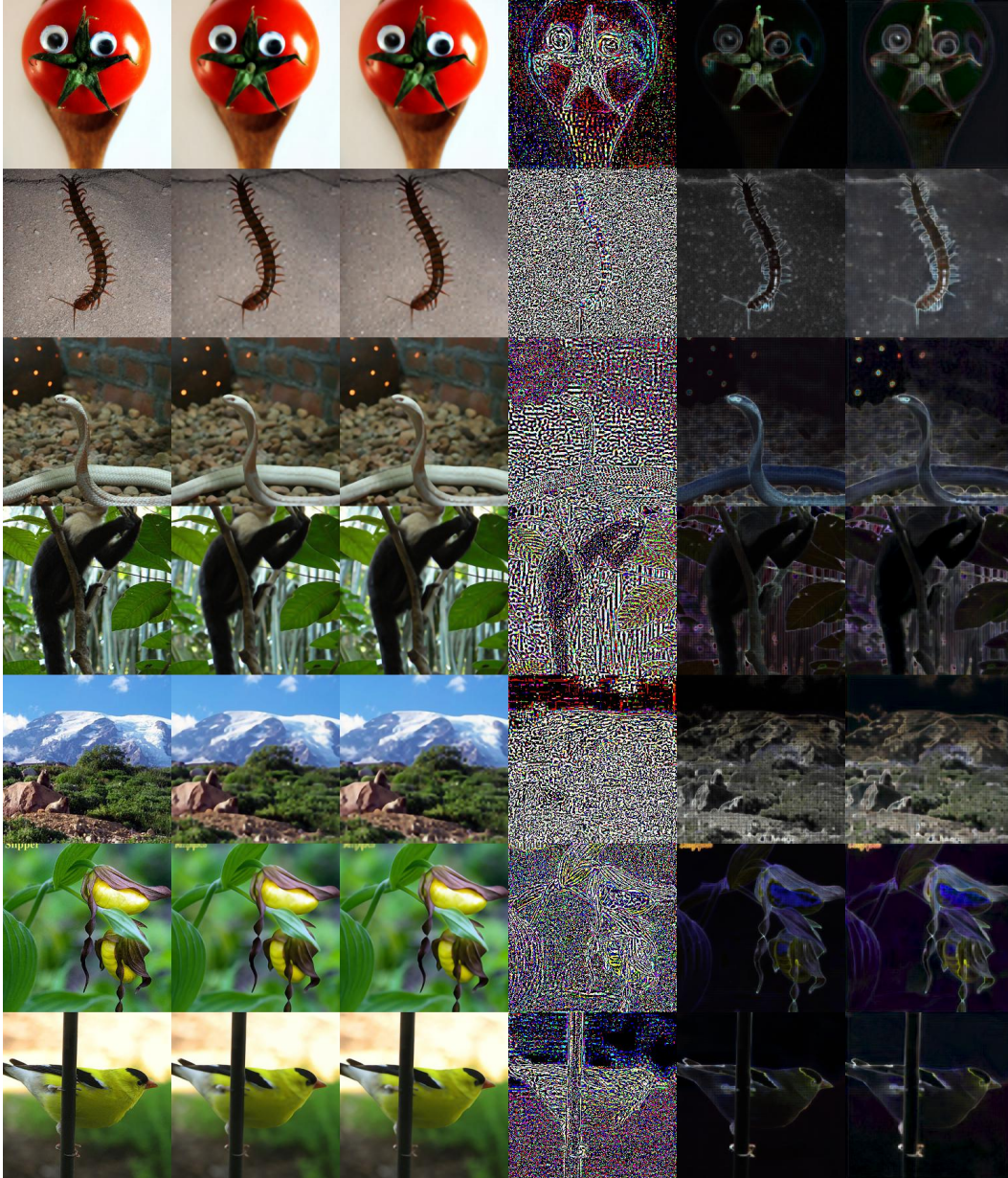


Figure 8: From left to right: the high-resolution image x (column 1); estimated $\mathbb{E}_{x|y}[x]$ by DDPM-SR; (column 2); estimated $\mathbb{E}_{x|y}[x]$ by f_{mean} (column 3); square root of label when training f_{var} , $|x - \mathbb{E}_{x|y}[x]|$ (column 4); estimated pixel-wise variance by DDPM-SR (column 5); estimated pixel-wise variance by f_{var} (column 6).

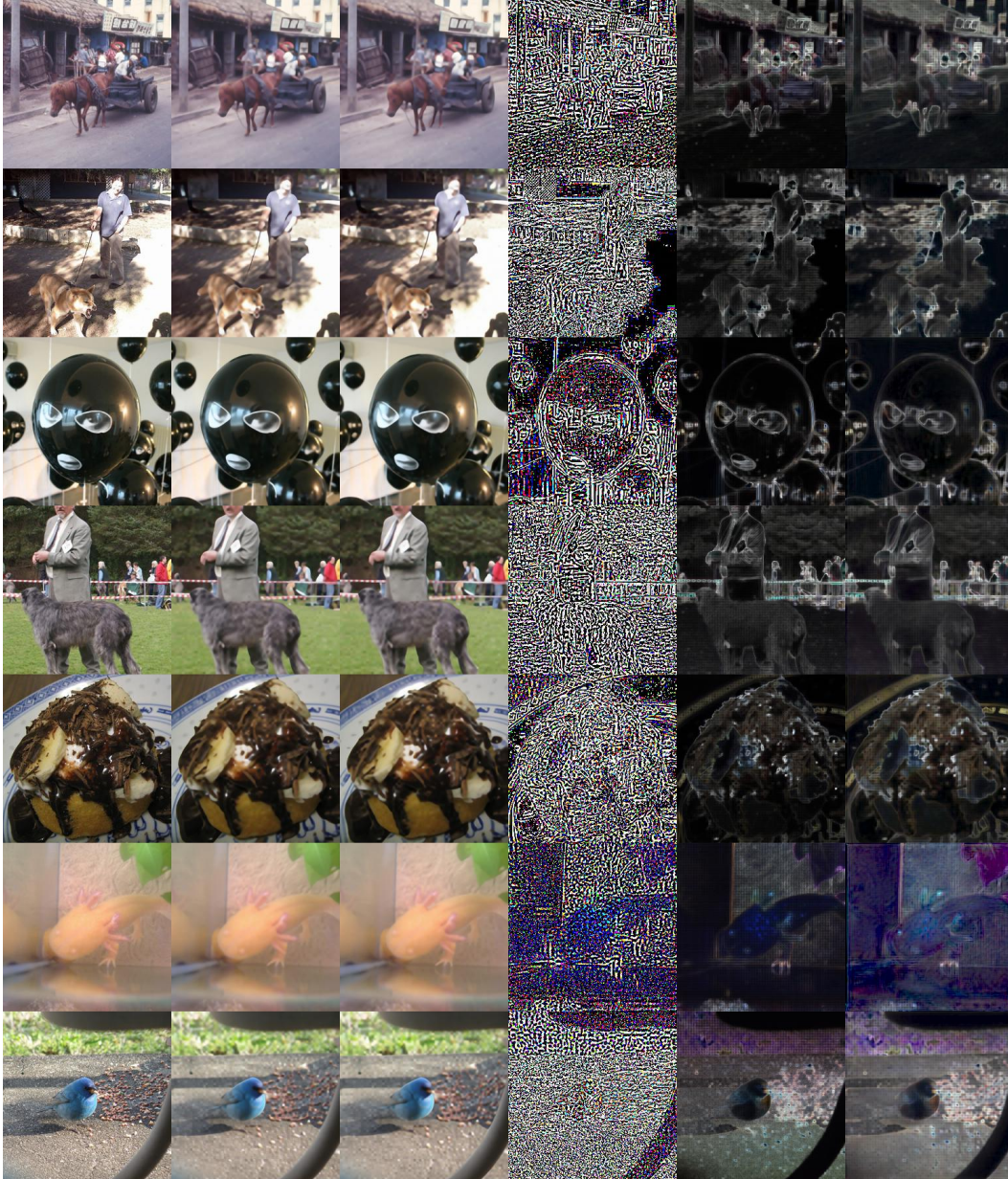


Figure 9: From left to right: the high-resolution image x (column 1); estimated $\mathbb{E}_{x|y}[x]$ by DDPM-SR; (column 2); estimated $\mathbb{E}_{x|y}[x]$ by f_{mean} (column 3); square root of label when training f_{var} , $|x - \mathbb{E}_{x|y}[x]|$ (column 4); estimated pixel-wise variance by DDPM-SR (column 5); estimated pixel-wise variance by f_{var} (column 6).

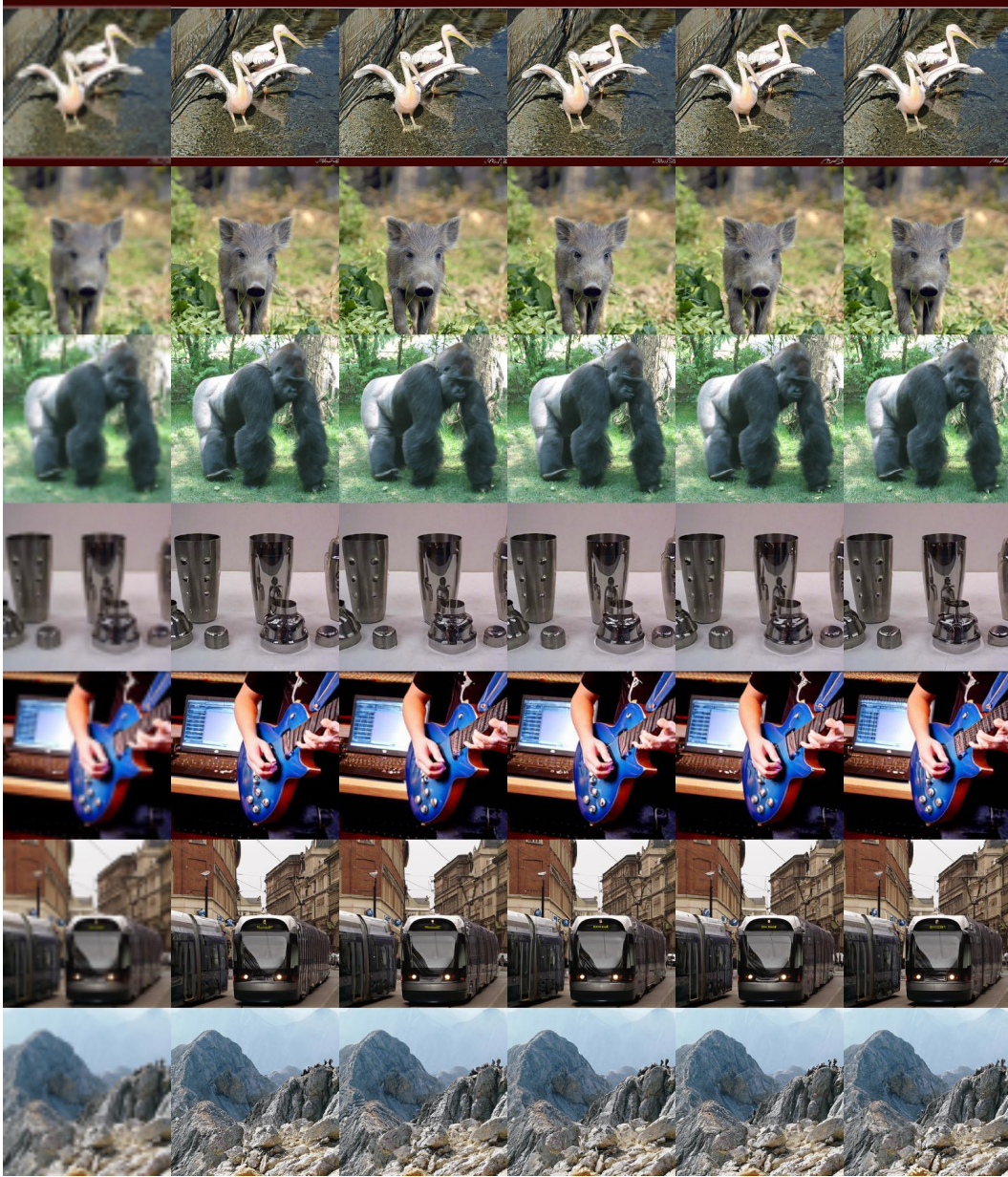


Figure 10: The first column is the upsampled low-resolution images from resolution of 64×64 to 256×256 . Other columns are high-resolution images generated by DDPM-SR. We can observe the difference of details among generated images, such as grass, rock, eyes, windows and so on.